Progress In Electromagnetics Research Letters, Vol. 55, 113–120, 2015

Design of Planar Dual-Band Branch-Line Coupler with π-Shaped Coupled Lines

Yu Cao, Jincai Wen*, Hui Hong, and Jun Liu

Abstract—In this paper, a planar microstrip branch-line coupler is designed to have dual-band operation. A Pi-typed structure is used in place of the conventional quarter wavelength transmission line for dual-band application. This structure consists of a pair of coupled line in which one has two ends while the other has open stubs attached to its two ends, and its circuit parameters are determined by the transmission line theory. Explicit design equations are derived using $ABCD$-matrix. For verification, a 3-dB branch line coupler with operating frequencies of 900 MHz and 3.5 GHz is fabricated and measured on an FR-4 printed circuit board (PCB). The simulated and measured results are in good agreement with each other.

1. INTRODUCTION

With the rapid progress of modern wireless communication systems, more and more dual- or multi-band RF and microwave subsystems are developed instead of the conventional structures for reducing system complicity, sharing the resources and cutting down the cost as much as possible. Up to now, various dual-band RF passive components have been designed and applied with theories and techniques, such as dual-band filters [1–3], power dividers [4, 5], crossovers [6, 7] and branch-line couplers [8–20].

Among dual-band couplers, there has been increasing interest in a dual-band branch-line coupler, which is useful in various microwave circuits, such as balanced amplifiers, balanced mixers, phase shifters and data modulators. A dual-band branch-line coupler was proposed using left-handed transmission lines [8]. However, in their realization, the lumped elements used in the circuit made significant losses, which restrict its practical application severely. The use of stub lines is very popular in obtaining the dual-band operation of the branch-line coupler [9–12]. In [9], a design was introduced by adding open- or short-circuit stubs tapped to the end of each branch line with simple design equations. Then, the dual-band operations were realized by open stubs tapped to the center of each branch line [10]. Stepped-impedance stubs were demonstrated to achieve more realizable frequency ratios and compactness [11, 12]. Ref. [13] demonstrates the design without any stubs or lumped elements, but its area is too large. Cross branch, which has additional freedom to utilize, was designed in dual-band couplers [14]. In the year of 2010, a new method was used with simple port extension [15]. Coupled lines are also used in achieving dual-band operations [16–19]. In [16], coupled lines were substituting for open stubs in T-shaped two-ports, which brought a complicated design and a narrow bandwidth. Refs. [17, 18] implemented the dual-band branch line coupler with only three coupled lines, which realized arbitrary coupling coefficient with compact size, but they did not give specific design procedure and the frequency ratio f_2/f_1 were restricted by the minimum gap spacing between the coupled lines.

In this article, a novel dual-band branch-line coupler is proposed. Each quarter wavelength section of a conventional branch-line coupler is replaced by the proposed elementary two-port which consists

Received 19 June 2015, Accepted 19 August 2015, Scheduled 27 August 2015

* Corresponding author: Jincai Wen (jcwencn@163.com).

The authors are with the Key Laboratory of RF Circuits and Systems, Education Ministry, Hangzhou Dianzi University, Hangzhou 310018, China.

of a pair of coupled lines and two open stubs attached to its two ends. This structure introduces more design freedom in the branch-line coupler to realize the desired dual-band operations. Design equations are formulated by establishing the equivalence between the π-shaped transmission lines and the quarter wavelength section at two operating frequencies with equal $ABCD$-matrix. For verification,a circuit operating at 900 MHz and 3.5 GHz is implemented by the standard PCB processes.

2. THEORETICAL ANALYSIS OF THE DUAL-BAND BRANCH-LINE COUPLER

Figure 1 shows the schematic diagram of the conventional branch line coupler. As said above, the key of dual band design is substituting the quarter wavelength branch line with an equivalent section that exhibits the desirable characteristics at two different frequencies.

The equivalent circuit consists of a pair of coupled lines in which one has two ends, and the other has open stubs attached to its two ends, as Figure 2 shows. Z_e, Z_o, θ_e and θ_o are the even- and odd-mode characteristic impedances and electrical lengths of the coupled lines, with Z and θ represent the characteristic impedance and electrical length of the open stubs, respectively. For the sake of analysis, the proposed structure is assumed to be reciprocal and lossless.

By applying a matrix formulation, the $ABCD$ parameters of the proposed three sections demonstrated in Figure 2(b) can be derived as

$$\begin{bmatrix} A_T & B_T \\ C_T & D_T \end{bmatrix} = \begin{bmatrix} 1 & 0 \\ j\tan\theta/Z & 1 \end{bmatrix} \begin{bmatrix} A_{coupler} & B_{coupler} \\ C_{coupler} & D_{coupler} \end{bmatrix} \begin{bmatrix} 1 & 0 \\ j\tan\theta/Z & 1 \end{bmatrix}, \tag{1}$$

where

$$A_{coupler} = D_{coupler} = \frac{\cos\theta_e \sin\theta_o (Z_e - Z_e \cos^2\theta_e) - \cos\theta_o \sin\theta_e (Z_o + Z_o \cos\theta_e \cos\theta_o)}{\sin\theta_e (Z_o \sin^2\theta_o - 2Z_o + Z_e \sin\theta_e \sin\theta_o)} \tag{2a}$$

$$B_{coupler} = j\frac{Z_o (Z_e \sin\theta_e + Z_o \sin\theta_o - 2Z_e \sin\theta_e \sin^2\theta_o)}{Z_o \sin^2\theta_o - 2Z_o + Z_e \sin\theta_e \sin\theta_o}, \tag{2b}$$

$$C_{coupler} = -j\frac{\begin{array}{l} -Z_e^2 \sin^2\theta_o + Zo^2 \sin^2\theta_e + Z_e^2 \cos^2\theta_e \sin^2\theta_o + Z_o^2 \cos^2\theta_o \sin^2\theta_e \\ +2Z_e Z_o \cos\theta_e \cos\theta_o \sin\theta_e \sin\theta_o \end{array}}{2Z_e Z_o \sin\theta_e (Z_o \sin^2\theta_o - 2Z_o + Z_e \sin\theta_e \sin\theta_o)} \tag{2c}$$

Although the phase velocity is different for even and odd modes, the assumption of equal electrical lengths ($\theta_e = \theta_o$) will be made for the following calculations.

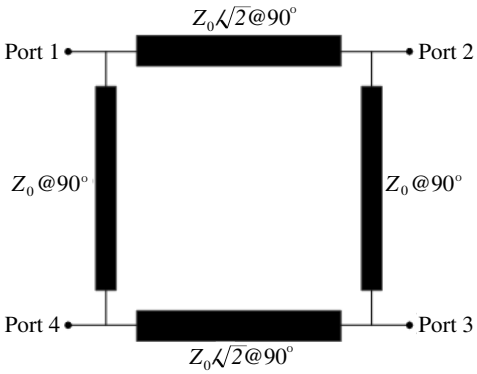

Figure 1. Traditional structure of branch-line coupler.

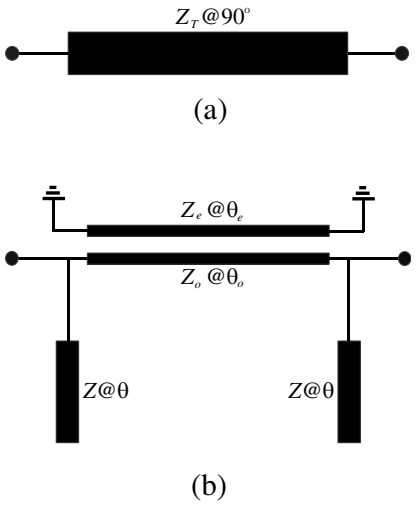

Figure 2. (a) Quarter wavelength branch. (b) Proposed structure.

For $\theta_e = \theta_o = \theta_x$, (1) becomes

$$\begin{bmatrix} A_T & B_T \\ C_T & D_T \end{bmatrix} = \begin{bmatrix} 1 & 0 \\ j\tan\theta/Z & 1 \end{bmatrix} \begin{bmatrix} \cos\theta_x & j2(Z_e//Z_o)\sin\theta_x \\ j\sin\theta_x/2(Z_e//Z_o) & \cos\theta_x \end{bmatrix} \begin{bmatrix} 1 & 0 \\ j\tan\theta/Z & 1 \end{bmatrix}. \quad (3)$$

By setting $Z_x = Z_e//Z_o$, each element of the $ABCD$-matrix is given by

$$A_T = D_T = \cos\theta_x - 2Z_x\sin\theta_x\tan\theta/Z \quad (4a)$$

$$B_T = j2Z_x\sin\theta_x \quad (4b)$$

$$C_T = j(\sin\theta_x/2Z_x + \cos\theta_x\tan\theta/Z + \tan\theta_x(\cos\theta_x - 2Z_x\sin\theta_x\tan\theta/Z)/Z) \quad (4c)$$

Since the proposed structure is equivalent to the conventional quarter-wavelength transmission line, the $ABCD$ matrix of the structure should equal that of a conventional section, yielding

$$\begin{bmatrix} A_T & B_T \\ C_T & D_T \end{bmatrix} = \begin{bmatrix} 0 & \pm jZ_T \\ \pm j/Z_T & 0 \end{bmatrix}, \quad (5)$$

where Z_T is the characteristic impedance of the conventional $\lambda/4$ line. The above expression leads to

$$Z = 2Z_x\tan\theta\tan\theta_x, \quad (6)$$

$$Z_x = \pm Z_T/2\sin\theta_x. \quad (7)$$

For the purpose of dual-band operation, the necessary conditions by (3) and (4) are

$$\sin\theta_{x1} = \pm 2Z_TZ_x \quad (8a)$$

$$\sin\theta_{x2} = \pm 2Z_TZ_x, \quad (8b)$$

$$\tan\theta_1\sin\theta_x = 2Z_TZ_x \quad (9a)$$

$$\tan\theta_2\sin\theta_x = 2Z_TZ_x, \quad (9b)$$

where θ_{x1}, θ_{x2}, θ_1 and θ_2 are electrical lengths of those lines at two desired operating frequencies.

The solution of (8) is

$$\theta_{x1} = n\pi - \theta_{x2}, \quad (10)$$

where $n = 1, 2, 3, \ldots$, and considering the relationship of

$$\frac{\theta_{x1}}{\theta_{x2}} = \frac{f_1}{f_2}, \quad (11)$$

As a result, once the two operating frequencies are chosen, the electrical lengths of the coupled line section will be determined as

$$\theta_{x1} = \frac{n\pi}{1 + \dfrac{f_2}{f_1}} \quad (12a)$$

$$\theta_{x2} = \frac{n\pi}{1 + \dfrac{f_1}{f_2}}. \quad (12b)$$

Combining (9a) and (9b), the electrical lengths for the shunt section (θ_1 and θ_2) can be computed following the same procedures for the coupled line as follows

$$\theta_1 = \frac{m\pi}{1 + \dfrac{f_2}{f_1}} \quad (13a)$$

$$\theta_2 = \frac{m\pi}{1 + \dfrac{f_1}{f_2}}, \quad (13b)$$

where $m = 1, 2, 3, \ldots$.

Finally, the design procedures of the proposed branch line coupler can be summarized as follows.

1) Considering the two operating frequencies (f_1 and f_2).

2) Using (12) and (13) to get the values of electrical lengths θ_{x1}, θ_{x2}, θ_1 and θ_2 at f_1 and f_2. For compactness, the values of n and m always equal 1.
3) Using (7) and the desired characteristic impedance (Z_T) to compute the value of Z_x.
4) Computing the value of Z by (6) combined with the parameters obtained in the former two steps.
5) Choose suitable Z_e and Z_o according to Z_x.
6) Computing the physical lengths of the coupled line and open stubs.

By replacing all four branch lines of the conventional coupler with the novel two-port structure, the topology of the whole new branch-line coupler is given in Figure 3.

Theoretically, the proposed coupler can operate at any two arbitrary frequency bands. However, in practice, the construction of the coupler is also constrained by the range of realizable impedance. Figure 4 gives the normalized values of Z and Z_x (with reference to Z_0) as a function of the frequency ratios f_2/f_1. These values are obtained from (6)–(7) with the branch electrical length obtained from (12)–(13) ($m = n = 1$). It can be found that the curve of Z rises with the decrease of the dual band ratio f_2/f_1. As f_2/f_1 approaches 1, the impedance of Z becomes infinite. Considering the realizable impedance values range from 20 to 120 Ω, a frequency ratio f_2/f_1 from 2.1 to 5.7 can be covered for a port impedance of 50 Ω. Meanwhile, the curve of Z_x rises with the increase of f_2/f_1. Since $Z_x = Z_e//Z_o$, for a certain Z_x, it is expected that there are infinitely solutions of Z_e and Z_o for dual-band requirement.

Without loss of generality, Z_e will be chosen as a freedom in design. Figure 4(b) shows the required two sets of even- and odd-mode impedances for the quarter-wave coupled-line sections against f_2/f_1. There are two practical limitations for those solutions. Firstly, it is necessary to ensure that Z_e is

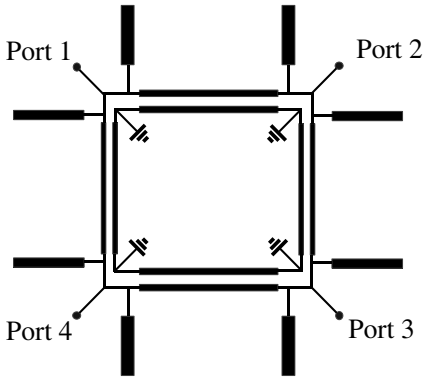

Figure 3. Final structure of the proposed coupler.

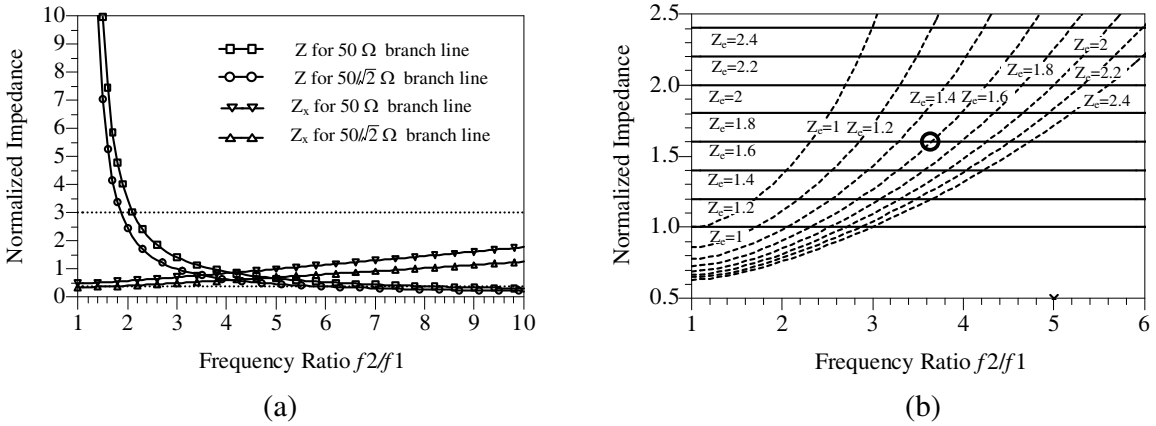

Figure 4. (a) Computed normalized branch-line impedances ($Z_0 = 50\,\Omega$) used in the dual-band coupler under different frequency ratio. (b) Required even- and odd-mode impedance versus frequency ratio.

greater than Z_o by a certain frequency ratio for a physically realizable coupled-line. For example, if Z_e is chosen to be 1.6, then the frequency ratio should be no larger than 3.63 (circle maker). Besides even-odd impedance relationship constraint, it is also necessary to consider whether the even- and odd-mode impedances are practical or not for a chosen circuit. Suitable values of Z_e and Z_o are required refer to the ultimate widths and gap spacing for a certain substrate technology. For there are various even and odd mode impedance Z_e and Z_o at certain two frequencies, it is convenient to utilize Z_e and Z_o to replace single line whose impedance values are out of practical range (20–120 Ω). What's more, different Z_{e} and Z_o lead to different bandwidth for certain dual-band f_1 and f_2. So suitable Z_o and Z_e can be chosen depending on various requirements.

3. SIMULATED AND MEASURED RESULTS

For verification, a proposed dual band microstrip branch-line coupler is simulated, fabricated and measured. $f_1 = 900\,\mathrm{MHz}$ and $f_2 = 3.5\,\mathrm{GHz}$ are selected as the operating frequencies. $\theta_x = \theta$ is chosen for simplified devising. From the design procedures above, the design parameters are derived and listed in Table 1.

Table 1. The design parameters of this prototype.

	50-Ω line	35.35-Ω line
Z_o, Z_e (Ω)	100, 71.61	75, 48.65
θ_x (deg in f_1)	36.8	36.8
Z	46.7	33
θ (deg in f_1)	36.8	36.8

For improved accuracy, the frequency response of the whole design including junction discontinuities and substrate effect was optimized by full-wave simulator and fabricated on the FR4-based PCB. The dielectric constant and the thickness of the substrate used are 4.6 and 0.8 mm. The loss tangent is 0.035. Images of the actual fabricated prototype is displayed in Figure 5. For compactness, the open stubs are all curled. Scattering parameter measurement were performed using Agilent 8719ES network analyzer over the frequency range from 0.5 to 4 GHz.

Figure 6 exhibits the simulated and measured results with close agreements obtained. It is found that the center frequency of the upper band slightly moves to 3.35 GHz. This deviation is possibly due to the fabricating error. Table 2 gives the performance of the proposed coupler. As Figure 6 and Table 2 shows, the magnitude of the return loss and the isolation loss are below −20 dB at 900 MHz and below

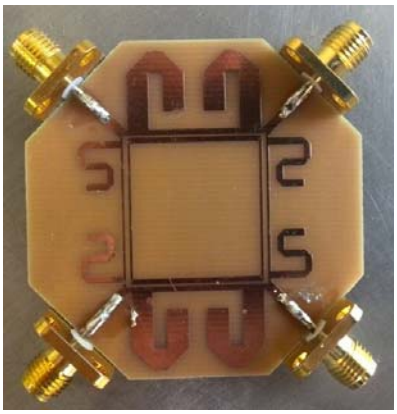

Figure 5. Photograph of the fabricated dual-band branch line coupler.

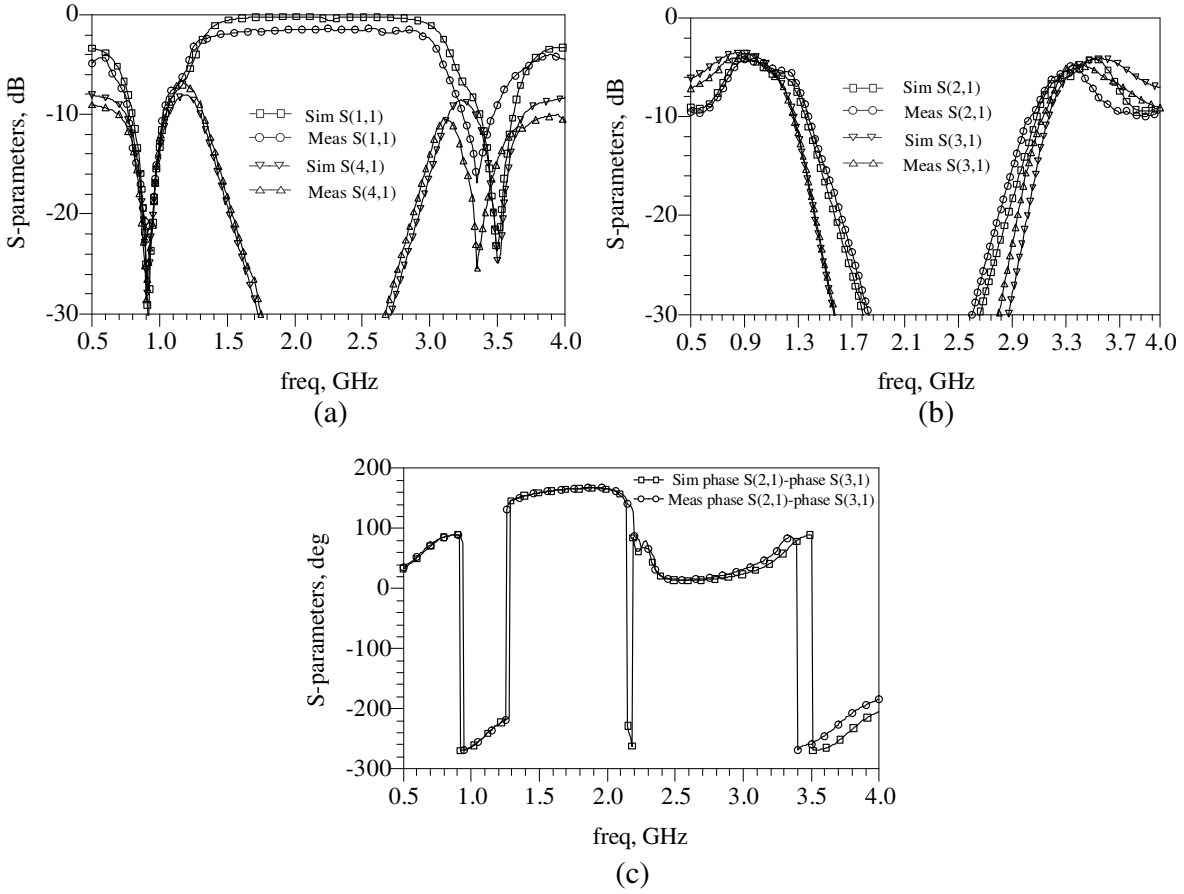

Figure 6. Simulated and measured results: (a) return loss $|S(1,1)|$ and isolation loss $|S(4,1)|$. (b) Insertion loss $|S(2,1)|$ and $|S(3,1)|$. (c) Output phase difference phase $S(2,1)$–phase $S(3,1)$.

-15 dB at 3.35 GHz, with the magnitude of the insertion loss $S(2,1) = -4.1$ dB, $S(3,1) = -4.2$ dB at 900 MHz and $S(2,1) = -4.6$ dB, $S(3,1) = -4.8$ dB at 3.35 GHz. It is apparently revealed that the loss at the upper frequency is higher than the lower frequency because of the lossy nature of FR-4 PCB. The phase differences between port 2 and port 3 (phase $S(2,1)$–phase $S(3,1)$) are 89.67° at 900 MHz and 86.13° at 3.35 GHz. Finally, the bandwidths of the designed branch line coupler are evaluated under the conditions of equal amplitude and quadrature phase difference. With the mismatches of amplitude and quadrature phase difference below 1 dB and 10°, two operating frequency bands are showed in Table 2.

Table 2. Measured results of the fabricated coupler.

Frequency	900 MHz	3.35 GHz
Input return loss ($\|S(1,1)\|$)	-22.5	-16.8
Isolation factor ($\|S(4,1)\|$)	-28.6	-25.4
Insertion loss ($\|S(2,1)\|$)	-4.1	-4.6
Insertion loss ($\|S(3,1)\|$)	-4.2	-4.8
Phase $S(2,1)$–phase $S(3,1)$	89.67	86.13
Relative bandwidth (Port 2)	23.33%	2.1%
Relative bandwidth (Port 4)	33.1%	6.57%

Table 3. Comparison of previously reported dual-band branch line coupler.

Reference	Operating frequencies (GHz)	1 dB-bandwidths (MHz)	Frequency ratio range f_2/f_1	FoM
[8]	0.92/1.74	140/110	–	–
[9]	0.9/2	200/110	1.8–3.7	0.57
[10]	0.9/2	130/130	1.25–2.85	0.48
[11]	2.4/5.8	336/464	1.7–2.7	0.35
[12]	2.4/5.2	300/201.4	1.1–6.3	0.94
[17]	2/4	100/130	1.5–3.2	0.176
[19]	0.95/1.52	230/180	1.5–1.76	0.423
This work	0.9/3.5	298/199.5	2.1–5.7	1.05

A comparison of the reported dual-band branch-line couplers and this work is summarized in Table 3. As there are numerous publications of the dual-band branch-line coupler, some represented works are included. In order to fairly compare the reported dual-band branch line couplers, a figure-of-merit (FOM) has been defined and described below:

$$FOM = \frac{(RBW_1 + RBW_2) \times \max(f_2/f_1)}{\min(f_2/f_1)}, \tag{14}$$

where RBW_1 and RBW_2 represent relative bandwidths of operating frequencies f_1 and f_2, respectively.

4. CONCLUSION

A new planar dual-band branch-line coupler is designed using four Pi-typed structures with coupled lines. The rigorous analysis of the structure is given by $ABCD$-matrix with exact design formulas derived in concise form. For the purpose of verification, a microstrip branch-line coupler of the proposed structure is constructed for 900 MHz and 3.5 GHz dual-band operation. Measured results demonstrate a slight frequency shift in upper band due to the fabrication tolerance. Moreover, for the lossy nature of FR-4 board, the actual loss at dual-band is higher than simulation results, especially at upper frequency. Nevertheless, the design structure in this article is useful for a variety of circuit or substrate technologies.

ACKNOWLEDGMENT

This work was supported by the National Natural Science Foundation of China under Grant 61372021 and 61331006.

REFERENCES

1. Chang, S.-F., Y.-H. Jeng, and J.-L. Chen, "Dual-band step-impedance bandpass filter for multimode wireless LANs," *Electronics Letters*, Vol. 40, 38–39, 2004.
2. Fan, J.-W., C.-H. Liang, and D. Li, "Design of cross-coupled dual-band filter with equal-length split-ring resonators," *Progress In Electromagnetics Research*, Vol. 75, 285–293, 2007.
3. Kamma, A., G. S. Reddy, R. S. Parmar, and J. Mukherjee, "Dual-band filter for WIMAX and WLAN with improved upper stop band performance," *Progress In Electromagnetics Research C*, Vol. 50, 131–138, 2014.
4. Park, M.-J. and B. Lee, "Wilkinson power divider with extended ports for dual-band operation," *Electronics Letters*, Vol. 44, 916–917, 2008.
5. Tang, X. and K. Mouthaan, "Compact dual-band power divider with single allpass coupled lines sections," *Electronics Letters*, Vol. 46, 688–689, 2010.

6. Lin, F., Q.-X. Chu, and S. W. Wong, "Dual-band planar crossover with two-section branch-line structure," *IEEE Transactions on Microwave Theory and Techniques*, Vol. 61, 2309–2316, 2013.
7. Shao, J., H. Ren, B. Arigong, C. Li, and H. Zhang, "A fully symmetrical crossover and its dual-frequency application," *IEEE Transactions on Microwave Theory and Techniques*, Vol. 60, 2410–2416, 2012.
8. Lin, I-H., C. Caloz, and T. Itoh, "A branch-line coupler with two arbitrary operating frequencies using left-handed transmission lines," *IEEE MTT-S International Microwave Symposium Digest*, Vol. 1, 325–328, 2003.
9. Cheng, K.-K. M. and F.-L. Wong, "A novel approach to the design and implementation of dual-band compact planar 90° branch-line coupler," *IEEE Transaction on Microwave Theory and Techniques*, Vol. 52, 2458–2463, 2004.
10. Zhang, H. and K. J. Chen, "A stub tapped branch-line coupler for dual-band operations," *IEEE Microwave and Wireless Components Letters*, Vol. 17, 106–108, 2007.
11. Chin, K.-S., K.-M. Lin, Y.-H. Wei, T.-H. Tseng, and Y.-J. Yang, "Compact dual-band branch-line and rat-race couplers with stepped-impedance-stub lines," *IEEE Transactions on Microwave Theory and Techniques*, Vol. 58, 1213–1221, 2010.
12. Zheng, N., L. Zhou, and W.-Y. Yin, "A novel dual-band Π-shaped branch-line coupler with stepped-impedance stubs," *Progress In Electromagnetics Research Letters*, Vol. 25, 11–20, 2011.
13. Wong, F.-L. and K.-K. M. Cheng, "A novel planar branch-line coupler design for dual-band applications," *IEEE MTT-S International Microwave Symposium Digest*, 903–906, 2004.
14. Park, M.-J. and B. Lee, "Dual-band, cross coupled branch line coupler," *IEEE Microwave and Wireless Components Letters*, Vol. 15, 655–657, 2005.
15. Kim, H., B. Lee and M. Joo, "Dual-band branch-line coupler with port extensions," *IEEE Transactions on Microwave Theory and Techniques*, Vol. 58, 651–655, 2010.
16. Atlasbaf, Z. and K. Forooraghi, "A new dual band branch-line coupler using coupled lines," *ISAPE'06. 7th International Symposium on Antennas, Propagation & EM Theory*, 1–4, 2006.
17. Yeung, L. K., "A compact dual-band 90 coupler with coupled-line sections," *IEEE Transactions on Microwave Theory and Techniques*, Vol. 59, 2227–2232, 2011.
18. Wang, X., W.-Y. Yin, and K.-L. Wu, "A dual-band coupled-line coupler with an arbitrary coupling coefficient," *IEEE Transactions on Microwave Theory and Techniques*, Vol. 60, 945–951, 2012.
19. Katakam, S., H. Ren, J. Shao, M. Zhou, B. Arigong, J. Ding, and H. Zhang, "A dual-band branch line coupler based on pi-shaped coupled lines," *Microwave and Optical Technology Letters*, Vol. 57, 501–504, 2015.
20. Collin, R. E., *Foundations for Microwave Engineering*, 2nd Edition, IEEE Press, New York, 1992.